INVESTIGATION OF WELD FAILURE IN SUPERAUSTENITIC UNS S31245 STAINLESS STEEL

B. DIXON
Ship Structures and Materials Division, Aeronautical and Maritime Research Laboratory, G.P.O. Box 4331 Melbourne, Victoria, Australia 3001

ABSTRACT

During the course of evaluating seam welded UNS S31254 superaustenitic stainless steel piping it was found that the parent metal gave up to 50 % tensile elongation values but some plasma-arc welded joints suffered weld metal cracking at elongation values as low as 10 %.

Scanning electron microscopy showed that the weld metal failed by low ductility, intercellular fracture along a network of brittle second phase particles having a composition similar to that of sigma (σ) phase. These particles were formed at the cell interfaces by transformation of delta ferrite during the final stages of solidification.

KEY WORDS

Superaustenitic stainless steel, sigma phase, plasma-arc welding, tensile straining.

BACKGROUND

UNS S31245 is a highly corrosion resistant, high strength austenitic stainless steel. It is one of a series of stainless steels often described as the '6 Mo superaustenitics' and was developed over 20 years ago as a possible replacement for conventional nickel-based alloys in the chemical processing, pulp and paper, food and drug industries where enhanced performance is required.

The steel provides substantially greater corrosion resistance and yield stress than the traditional 300 series austenitic stainless steels due to its high alloy content (including 0.2%N). Typically the composition is 0.01% C, 0.45% Si, 0.51% Mn, 20.1% Cr, 17.5% Ni, 6.1% Mo, 0.2% N, 0.72% Cu and balance Fe.

During tensile testing of samples cut from 3 mm thick UNS S31254 piping it was found that parent metal gave elongation values of about 50 % and UTS values in the order of 720 MPa. However, plasma-arc welded seam joints showed significant cracking at strains in the range of 12 to 23 %. Detail of one tensile test specimen showing extensive cracking in the weld region is provided in Figure 1. It was of concern that this relative low ductility may be a cause of weld zone cracking during cold working processes such as pipe bending.

The purpose of this investigation was to identify the causes of failure in these welds and to evaluate the risk and likely consequences of such cracking on the performance of piping manufactured from the material.

2 EXPERIMENTAL WORK

A series of six tensile tests was carried out on metal containing welds and a further two tests were carried out on unwelded metal. At intervals during each test, the straining was stopped in order to inspect the specimen with the aid of a travelling microscope and to count the number of cracks evident on the surface. The extent of cracking in both the weld metal and weld heat affected zone (HAZ) was recorded.

Figure 1 Central region of a flat dumbell type tensile specimen of UNS 31245 stainless steel having a plasma arc weld down the centre. The test has been arrested after approximately 21% elongation. This specimen shows a large transverse crack (large arrow) in the weld and a number of smaller cracks (small arrows) at the weld toes.

Scanning electron microscopy of fracture surfaces was undertaken by continuing the tensile test to failure and inspecting the resulting surface. The weld deposits were also inspected metallographically using electrolytic and colour deposition etching techniques.

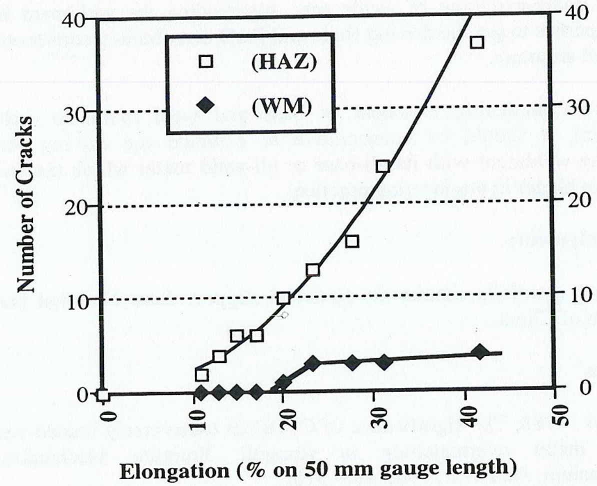

Figure 2 Extent of surface cracking in the weld and heat affected zones during tensile testing of one specimen. The number of HAZ cracks increased exponentially as straining was applied.

3 RESULTS

Results of tensile testing for one plate are shown in Figure 2. It is evident that HAZ cracking initiated after about 10% elongation and that the number of cracks increased as the tensile strain was increased. All of the welded plates showed a similar behavior. The unwelded plates showed no evidence of cracking up to failure at 49% elongation.

The weld metal microstructure (Figure 3) shows a cellular structure with grain boundaries at the cell interfaces. Other regions of the weld showed cellular and cellular-dendritic microstructures. There was no evidence of grain boundary straightening at any region of the weld.

Figure 4 shows that the parent metal underwent significantly greater plastic deformation during fracture than the weld metal. Details of the fracture surface (Figure 5) showed that the weld metal had small dimples typical of low ductility fracture. It was also evident that fracture occurred along the cell interfaces because the surface clearly has a cellular appearance. At higher magnifications, the weld metal fracture surface (Figure 6) was seen to be covered by a brittle film which had apparently broken up into particles. A number of these particles were analysed by energy dispersive X-ray analysis (EDXA) in the electron microscope and, by comparison with the parent metal, they were enriched in the elements silicon, molybdenum, and chromium and depleted in the elements iron and nickel.

Electron microprobe analysis (EPMA) across a segregate at the plate centerline has been undertaken and the trace (Figure 7) showed a clear enrichment in the elements chromium, molybdenum and silicon at the segregate phase combined a depletion in the elements iron and nickel. Quantitative analysis of the matrix material and second phase is presented in Table 1.

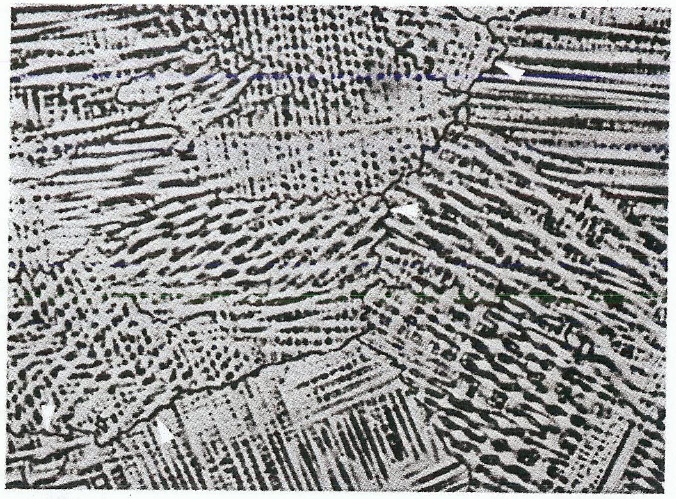

Electrolytic oxalic acid etch. X200

Figure 3 Microstructure of region in weld showing grain boundaries (arrowed) at the cell interfaces.

4 DISCUSSION

The transverse cracking induced by tensile strain is extensive (e.g. see Figure 2). Inspection of the fracture surface in Figure 4 shows that it is largely confined to the weld zone and is associated with minimal surface deformation. Where cracking has extended into the parent metal, the crack growth is associated with significant deformation, suggesting that the weld metal has low ductility compared with the parent metal.

Figure 5 confirmed that failure occured by low ductility fracture and also illustrated that the weld metal fracture path occurs along cell interfaces, that is, at the location where grain boundaries were found in the metallographic section (Figure 3). This suggests that either cell interfaces or grain boundaries offered the easiest path for crack growth.

Metallographic sections across a number of welds showed a pronounced segregation at the plate centreline. The segregate was found by EPMA (Table 1) to be enriched in the ferrite promoting elements; Cr, Mo and Si, and depleted in the austenite formers; Fe and Ni. It was similar in composition to the second phase particles on the weld fracture surface. This composition range is close to the sigma (σ) phase which is known (Castro R. and de Cadenet J.J. [i]) to be associated with high proportion of ferrite formers in the weld metal. Furthermore, (Castro R. and de Cadenet J.J. [i]) high molybdenum and silicon contents have the effect of expanding the temperature range over which sigma phase exists.

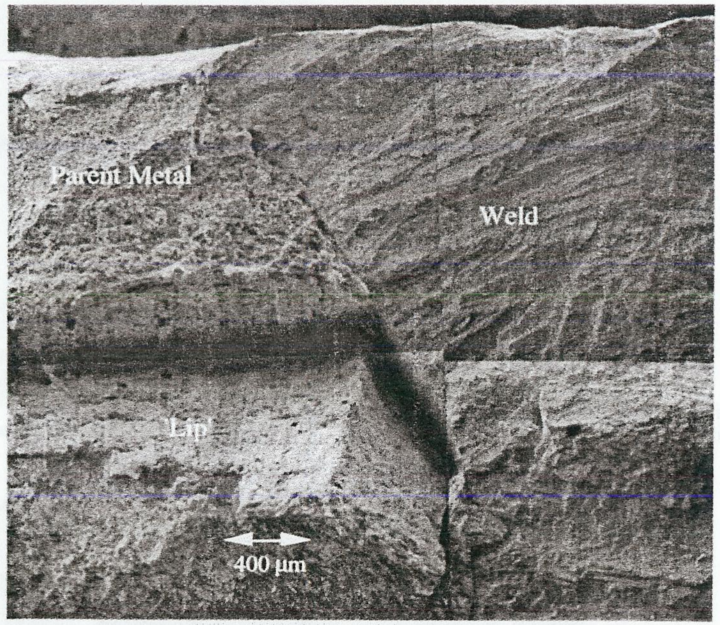

Figure 4 Scanning electron micrograph of a fracture surface. The parent metal shows ductile fracture while the weld metal has low ductility. In this specimen, the plate also opened along it's centreline at the region marked 'lip' in this image.

Sigma phases are hard and brittle and, if present in significant amounts, can have the effect of increasing hardness and reducing toughness of the weld deposit (Castro R. and de Cadenet J.J. [i]).

According to the welding procedure, the welds in these plates were undertaken using single pass plasma-arc welding with a travel speed of 600 - 800 mm/min. The welds were subsequently soaked at 1150 - 1180°C for 5 - 8 minutes and then quenched by water spraying.

Throughout the weld cross section the structure was mainly cellular, as shown in Figure 3, however there was some cellular-dendritic solidification. This microstructure here is representative of weld metals that have undergone rapid solidification, as in plasma arc welding. It is noteworthy, that these grain boundaries travel along the cell interfaces; that is, there has been little grain boundary straightening or grain growth in the weld. This is unusual because, under the welding procedure described above, it might be expected that the grain boundaries would straighten during cooling after the welding process, and that the subsequent soaking treatment would cause significant grain growth.

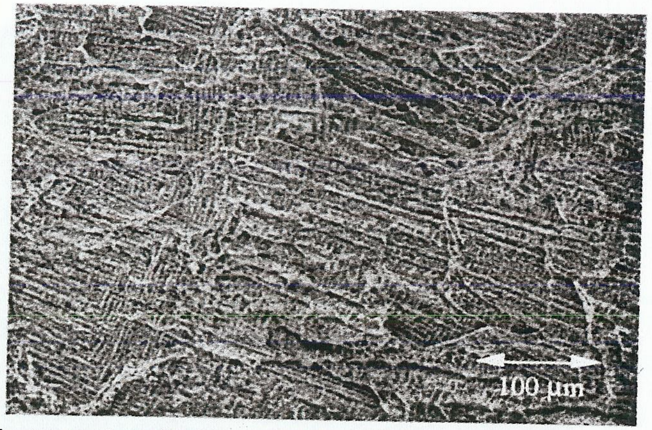

Figure 5 Fracture surface of weld metal in Figure 4. The fracture appearance is low ductility dimples with fracture along cell interfaces.

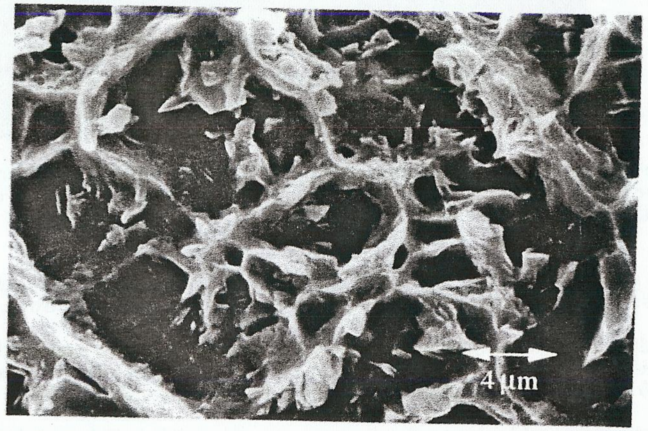

Figure 6 Detail of weld fracture surface (Figure 5) showing that surface is covered with remnants of a brittle film.

An explanation for this is that a segregate phase has formed at the cell interfaces during solidification and that this second phase has pinned the grain boundaries. Such a segregate would need to form during the final stages of weld solidification. Koseki, T. and Ogawa, T. ii describe a mechanism by which interdendritic ferrite transforms to sigma phase during the final stages of solidification in stainless steels similar to those studied here.

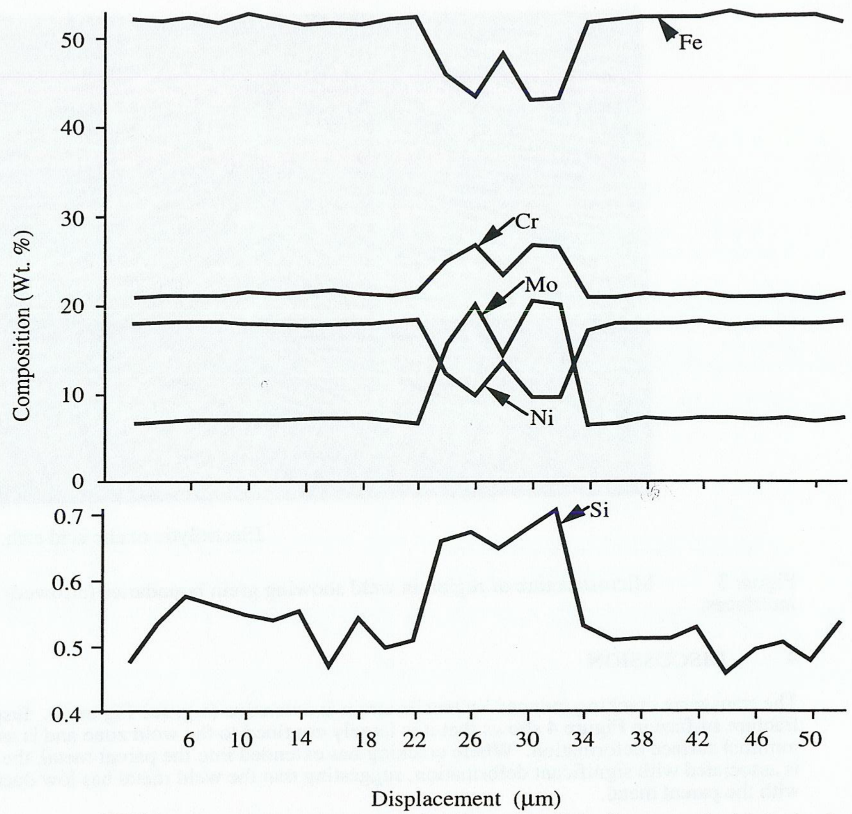

Figure 7 EPMA trace across a segregate at the plate centreline. Segregate is rich in the ferrite promoting elements; chromium, molybdenum and silicon and it is depleted in the austenite promoting elements; iron and nickel. The composition is similar to that of sigma phase.

Close examination of the weld and 'lip' surfaces (Figure 4) shows that both were covered with brittle particles that appear to be remnants of a surface film. Particles of similar appearance were identified as brittle films on duplex stainless steels in Vilpas, M. and Ruusila, R. [iii]. The compositions of the particles were similar to each other in the (non-quantitative) EDXA analysis and it was deduced that the weld surface film was largely composed of similar second phase material.

It is therefore concluded that the weld cracking and brittleness identified here is caused by the existence of brittle second phase particles, including sigma phase, in the weld deposit. It seems that the second phase resulted from segregation of ferrite forming elements during the final stages of solidification. The second phase material formed a discontinuous network through the weld zone and provided a low-ductility path for the growth of cracking under strain loading.

Investigations have been undertaken to study the fitness-for-purpose of these welds in terms of their resistance to fatigue and shock loading. It might be assumed however that the existence of brittle, second phase networks within the weld deposits would render any piping unfit for use in critical applications where shock and fatigue loading is experienced; regardless of the extent of cracking, or even if the welds contain no cracking. For other applications it might be acceptable to use the welded material provided that the weld joint is subjected to 10% strain or less. For welded piping this might be achieved by ensuring that the weld seam is located close to the neutral axis.

Table 1 Composition of matrix and second phase material (See Figure 7)

Element	Matrix		2nd. Phase	
	(Wt, %)	(Atom, %)	(Wt, %)	(Atom. %)
Mn	0.5	0.53	0.52	0.6
Si	0.55	1.1	0.9	1.9
Cr	20.3	22.4	25.7	29.7
Ni	17.8	17.4	10.5	10.8
Mo	6.2	3.7	18.6	11.6
Fe	53.5	54.9	42.2	45.3
Nb	0.03	0.02	0.08	0.05
Ti	0.002	0.004	0.02	0.04

CONCLUSIONS

1 Extensive transverse cracking can occur in longitudinal seam welds on plasma arc welded UNS S31254 stainless steel tensile test plates. Such cracking occurs at levels of strain greater than 10%.

2 Cracking is associated with the existence of brittle second phases, including sigma phase, in the weld deposit.

3 The weld deposits investigated have low ductility and there exists a significant risk of cracking in service where conditions involve fatigue or shock/impact loading.

ACKNOWLEDGEMENTS

Preparation of specimens for this work was undertaken by Nick Baldwin, Ian Jackson, Paul Calleja and Gavin Ryan. Electron microscopy was done by John Russell.

REFERENCES

i Castro R. and de Cadenet J.J. (1975) 'Welding Metallurgy of Stainless and Heat-Resisting Steels' Cambridge University Press

ii Koseki, T. and Ogawa, T., (1991) 'An Investigation on the Weld Solidification of Cr-Ni-Fe-Mo Alloys', J. Jap. Weld. Soc., 9, 1, 143-149.

iii Vilpas, M. and Ruusila, R. (1993) 'Welding of Superduplex Stainless Steels' Svetsaren, 47, (2), 26